PHYSICAL REVIEW B VOLUME 59, NUMBER 23 15 JUNE 1999-I

Mixed-valence states in narrow-gap IV-VI semiconductors with rare-earth ions

V. K. Dugaev and V. I. Litvinov*
Chernovtsy Department of the Institute of Materials Science Problems, 5 Vilde Street, Chernovtsy 274001, Ukraine

A. Łusakowski
Institute of Physics, Polish Academy of Sciences, Al. Lotników 32/46, 02-668 Warszawa, Poland

(Received 10 August 1998)

The mechanism of valence-state formation in the IV-VI alloys doped with rare-earth impurities is analyzed with respect to certain properties of narrow-gap semiconductors. The mean-field approximation in the slave-boson representation is used to account for the strong electron correlation at the impurity. The energy, width, and filling factor of the impurity level are calculated as a function of both the band gap and position of the chemical potential. We also calculate the temperature dependence of the magnetic susceptibility of an impurity. It is shown that mixing to coupled conduction- and valence-band states makes the properties of rare-earth dopants sensitive to the band gap and Fermi level in the narrow-gap semiconductor host.

[S0163-1829(99)08723-8]

I. INTRODUCTION

The problem of a mixed valence in metals doped with rare-earth atoms has been investigated for a long time. The intermediate valence or mixed-valent state has been rigorously established (see, for example, review articles[1–4] and references therein). In metals, the behavior of rare-earth impurities is not, generally, very sensitive to a host material, but mostly depends on the specific kind of rare-earth impurity and relative position of the deep impurity level and Fermi level.[5]

Recent experiments on rare-earth-doped narrow-gap IV-VI semiconductors revealed the variable valence state of Yb for which the *f* level is located deeply in the valence band of the host material.[6–8] In Yb-doped $Pb_{1-x}Ge_xTe$ crystals, a switch between Yb^{2+} and Yb^{3+} states was established, when the chemical potential moved within the valence band. Such a change of the Yb impurity state is attributed to a change of the filling of the *f* shell at the Yb ion: from 14 electrons in the neutral state (Yb^{2+}) to 13 electrons in the ionized one (Yb^{3+}).

The situation in narrow-gap semiconductors differs from that of metals in some aspects. First, the coupling between conduction and valence bands, which causes the nonparabolicity of the energy spectrum, gets a mixing between the *f* level and the valence band influenced by conduction-band states. The admixture of the conduction-band states makes the mixed-valence behavior of the dopant dependent on the energy gap. Second, the Fermi-level position depends on carrier density; thus, the basic magnetic properties of rare-earth-doped narrow-gap materials have to be sensitive to growth conditions and annealing when native defects and impurities other than rare-earth ones strongly influence the carrier concentration. All this implies that the mixed-valence behavior of the narrow-gap semiconductors has to be considered in more detail with respect to peculiarities of the energy spectrum and the sensitivity of the material to external conditions.

Impressive progress in the theory of mixed states has been achieved in the framework of the slave-boson field theory and the $1/N$ expansion.[9–12] Use of a slave-boson technique enables one to account for the strong Coulomb correlation at the impurity center, whereas the $1/N$ expansion essentially simplifies all the calculations, reducing them to a kind of mean-field approximation, with small fluctuations around a mean-field solution.

In this paper we consider the theory of the mixed-valence state in degenerated IV-VI narrow-gap semiconductors. As a tool, we use the slave-boson technique and $1/N$ expansion, approaches which have been successful in the case of metals.

We are going to apply these approaches to the IV-VI narrow-gap semiconductors, such as PbTe or $Pb_{1-x}Sn_xTe$ alloys, and to take into account peculiarities of the wave functions and energy spectrum of these compounds.[13] In IV-VI semiconductors, in each of four valleys there are two close bands separated by a small energy gap. Only small volumes of the *k* space in each valley are allowed for electrons and holes, namely, in vicinities of *L* points of the Brillouin zone. The electron density of states is small within each valley due to the small effective masses of carriers. It means that the total probability of electron transitions between a localized and band states should be rather small.

The basis wave functions near band edges in IV-VI compounds allow the interband coupling which causes nonparabolicity of the energy spectrum. The amplitude of the electron wave function at a cation site is much larger than that of the hole wave function. This makes the s-d interaction of localized electrons with the conduction band larger than that with the valence band; thus, the mixing of the localized electrons with valence band is mostly indirect due to virtual conduction-band states. In IV-VI semiconductors the rare-earth impurity substitutes the metal (cation) site in IV-VI binary compounds, which results in a strong mixing between conduction-band states and deep localized levels even in degenerated crystals such as p-PbGeTe(Yb).

Strictly speaking, the s-d coupling constants depend on the specific type of energy valley. If we direct the quantization axis along a distinguished vector of a certain valley, then

©1999 The American Physical Society

the overlap integrals will be different for this valley and for other equivalent tilted valleys (the wave function of carriers at the band edge have spherical symmetry, whereas the localized impurity has orbital moment $l=3$). For the sake of simplicity, we are going to neglect this anisotropy and consider the coupling constants as parameters independent of valley number. The possible justification is that the contribution from three equivalent tilted valleys is larger than that from one certain valley. We neglect also the anisotropy of the energy spectrum in order to avoid the necessity of coordinating the anisotropy axis of each valley with the quantization axis. Actually, the final result is always reached after summation over all valleys, which results in a corrected interaction parameter that is just the mean geometrical value of transverse and longitudinal s-d interaction constants.

It should be noted that the variable valence in the IV-VI semiconductors doped with third-group impurities In and Tl was discussed earlier by several authors, mostly with regards to the persistent photoconductivity[14,15] and superconductivity.[16]

II. MODEL

The model takes into account two-band electrons with interband coupling and spin-orbit interaction in each energy valley. The interaction of band electrons with localized ones is taken in the form of Anderson hybridization, with inclusion of a slave-boson field b_{am}, where the indices a and m indicate the valley and magnetic quantum numbers ($m=l,l-1,...,-l$, and $l=3$ for Yb), respectively.

The Hamiltonian of the model has the form

$$H=\sum_{ka}\psi^{\dagger}_{ka}\hat{\epsilon}_k\psi_{ka}+\sum_{m}c^{\dagger}_{m}\epsilon_0 c_m$$
$$+\sum_{kam}[\psi^{\dagger}_{ka}\hat{V}_k c_m b_{am}+c^{\dagger}_{m}b^{\dagger}_{am}\hat{V}_k\psi_{ka}], \tag{1}$$

where ϵ_0 is bare the energy level of an f electron at the impurity atom. The matrix in space of bands and spins of the Dirac model for the electron energy spectrum in IV-VI crystals $\hat{\epsilon}_k$ is given as[13]

$$\hat{\epsilon}_k=\begin{pmatrix}\Delta & v\mathbf{k}\cdot\sigma\\ v\hat{\mathbf{k}}\cdot\sigma & -\Delta\end{pmatrix}, \tag{2}$$

where 2Δ is the energy gap and v is the interband coupling parameter. The energy spectrum in conduction (c) and valence (v) bands is $\omega_{1,2}=\pm E_k=\pm(\Delta^2+v^2k^2)^{1/2}$. In accordance with Eq. (1), the transitions of an electron from a band to a localized f state (and vice versa) is accompanied by processes of emission and absorption of a boson b_{am}.

Here the basis functions for free electrons of each valley, localized f electrons, and slave bosons are taken as spinors in space of bands (c,v) and spin states:

$$\psi^{\dagger}_{ka}=(\psi^{\dagger}_{kac\uparrow},\psi^{\dagger}_{kac\downarrow},\psi^{\dagger}_{kav\uparrow},\psi^{\dagger}_{kav\downarrow}),$$
$$c^{\dagger}_{m}=(c^{\dagger}_{m\uparrow},c^{\dagger}_{m\downarrow}),\quad b^{\dagger}_{am}=(b^{\dagger}_{amc},b^{\dagger}_{amv}). \tag{3}$$

$\hat{V}_k$ is the diagonal matrix in the space of bands:

$$\hat{V}_k=w(k)*\begin{pmatrix}V_1 & 0\\ 0 & V_2\end{pmatrix},$$

where V_1 and V_2 are hybridization coupling constants to the conduction and valence bands. The hybridization [last term in Eq. (1)] generates s-d scattering from the localized impurity (Fig. 1):

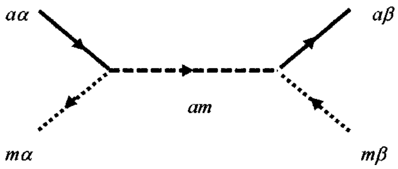

FIG. 1. Band-impurity coupling via a slave-boson b field (solid line, free electrons: dots, localized electron: dashed lines, b field).

$$H_{\text{int}}=J\sum_{kk'a\alpha\beta}\psi^{\dagger}_{ka\alpha}c^{\dagger}_{m\beta}c_{m\alpha}\psi_{k'a\beta}, \tag{4}$$

as follows from the second-order perturbation over $\hat{V}_k$. Here α and β are the spin indices.

The condition that the localized center can contain not more than one hole can be expressed by an additional equation

$$\sum_{ami}b^{\dagger}_{ami}b_{ami}+\sum_{m}\tilde{c}^{\dagger}_{m}\tilde{c}_{m}=1, \tag{5}$$

where $\tilde{c}^{\dagger}$ and $\tilde{c}$ are the creation and annihilation operators for holes at the f state. Equation (5) means that we consider a nearly filled f shell that corresponds well to the case of Yb impurities. With this constraint, the free energy of the system is given as

$$F=\int_0^{\beta}d\tau\Bigg\{\sum_{ka}\psi^{\dagger}_{ka}\left(\frac{\partial}{\partial\tau}+\hat{\epsilon}_k\right)\psi_{ka}+\sum_{m}\tilde{c}^{\dagger}_{m}\left(\frac{\partial}{\partial\tau}-\epsilon_0+\lambda\right)\tilde{c}_m$$
$$+\sum_{am}b^{\dagger}_{am}\left(\frac{\partial}{\partial\tau}+\lambda\right)b_{am}+\sum_{kam}(\psi^{\dagger}_{ka}\hat{V}^{\dagger}_{k}c_m b_{am}$$
$$+c^{\dagger}_{m}b^{\dagger}_{am}\hat{V}_k\psi_{ka})-\lambda\Bigg\}, \tag{6}$$

where $\beta=1/T$ and τ is the thermodynamic time.[17] The partition function of the system,

$$Z=\int D\psi^{\dagger}_{ka}D\psi_{ka}Dc^{\dagger}_{m}Dc_{m}Db^{\dagger}_{am}Db_{am}D\lambda\, e^{-F}, \tag{7}$$

includes the integration over the $\lambda(\tau)$ field, entering the free energy as a Lagrange factor.

If we integrate out $b^{\dagger}$ and b fields, we come to a four-particle interaction of the form of Eq. (4) with $J\sim(V_1^2+V_2^2)/(\lambda-\epsilon_0)$. It should be noted that using a b field with a magnetic momentum projection m and valley index a allows us to model the hybridization interaction and implies that the scattering of a free carrier from impurity (4) conserves the total magnetic momentum and intervalley scattering is absent.

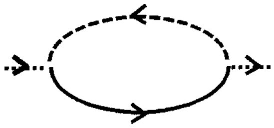

FIG. 2. Loop diagram containing the large factor N_a.

III. CONDENSATION OF SLAVE BOSONS

The thermodynamical Green functions are defined as[17]

$$G_{ka}(\tau,\tau')=-\langle T_\tau \psi_{ka}(\tau)\psi^\dagger_{ka}(\tau')\rangle,$$

$$G_f(\tau,\tau')=-\langle T_\tau c_j(\tau)c^\dagger_j(\tau')\rangle,$$

$$D_{ami}(\tau,\tau')=-\langle T_\tau b_{ami}(\tau)b^\dagger_{ami}(\tau')\rangle, \tag{8}$$

where G_{ka}, G_f, and D_{ami} are Green functions of free carriers, localized electrons, and b bosons, respectively. The bare Green functions after Fourier transformation to the imaginary frequencies are given as

$$G^0_k(i\epsilon)=\frac{i\epsilon+\mu+\tau_z\Delta+\tau_x v\sigma\cdot\mathbf{k}}{(i\epsilon+\mu)^2-E_k^2},$$

$$G^0_f(i\epsilon)=\frac{1}{i\epsilon-\epsilon_R+\mu},\quad D^0_{ami}(i\omega)=\frac{1}{i\omega-\lambda}, \tag{9}$$

where τ_x and τ_z are the Pauli matrices, $\epsilon_R\equiv\epsilon_0-\lambda$ is the renormalized impurity level, and μ is the chemical potential. Here the discrete frequencies are $i\epsilon=(2n+1)\pi T$ for fermions and $i\omega=2n\pi T$ for b bosons.

Consider now the diagrams for the impurity Green function $G_f(i\epsilon)$. Diagrams with closed loops (Fig. 2) are proportional to N_a (number of valleys). We assume $N_a\gg 1$; this allows us to take into account only loop diagrams and corresponds to the $1/N$ expansion.[12] The self-energy operator for the impurity Green function is (Fig. 3)

$$\Sigma_f(i\epsilon)=-N_aT\sum_{nki}V_iG^0_{ki,kj}(i\epsilon_n)V_jD_{ji}(i\epsilon_n-i\epsilon), \tag{10}$$

where G and D are written as i and j elements of the corresponding matrix Green functions.

The integration over momentum of the matrix G^0_k in Eq. (10) gives zero for nondiagonal terms; thus, we get

$$\Sigma_f(i\epsilon)=-N_aT\sum_{nki}V_i^2G^0_{ki}(i\epsilon_n)D_i(i\epsilon_n-i\epsilon). \tag{11}$$

The onset of the intermediate valence in this approach corresponds to condensation of the boson b field. The density of condensates, $\varphi_i=\langle b_i^\dagger b_i\rangle$, determines the shift and width of the impurity level in the mixed-valence state. In the condensed state the boson Green function $D_i(i\epsilon)\sim\delta(i\epsilon)$. So we can replace $G^0_{ki}(i\epsilon_n-i\epsilon)$ by $G^0_{ki}(i\epsilon)$ in Eq. (11), and use the relation $\varphi_i\equiv-D(\tau,\tau+\delta)=-T\Sigma_n\exp(i\omega_n\delta)D_i(i\omega_n)$. Equation (11) can be written as

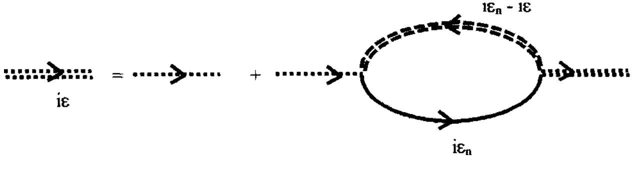

FIG. 3. Dyson's equation for the impurity Green function.

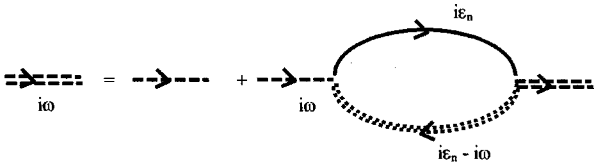

FIG. 4. Dyson's equation for the b-boson Green function.

$$\Sigma_f(i\epsilon)=-iN_a\sum_i\varphi_i\Gamma_i(i\epsilon), \tag{12}$$

where

$$\Gamma_i(i\epsilon)=i\sum_k V_i^2G^0_{ki}(i\epsilon). \tag{13}$$

The boson Green function $D_i(i\omega)$ will be found from Dyson's equation (Fig. 4) $D_i^{-1}=(D_i^0)^{-1}-\Pi_i$, where

$$\Pi_i(i\omega)=T\,\mathrm{Sp}\sum_{nk}V_i^2G^0_{ki}(i\epsilon_n)G_f(i\epsilon_n-i\omega) \tag{14}$$

is the polarization operator and the trace goes in the spin space. Using Eqs. (12)–(14), we find the condition for condensation of the i-boson field b_i $(\lambda+\Pi_i=0)$ in the form

$$-2iT\sum_n\frac{\Gamma_i(i\epsilon_n)}{i\epsilon_n-\epsilon_R+\mu+iN_a\Sigma_j\varphi_j\Gamma_j(i\epsilon_n)}+\lambda=0. \tag{15}$$

Equation (15) contains different Γ_i; thus, we have different conditions for condensation of b_i fields. This means that condensation is possible for both $i=1,2$ boson fields separately. Such asymmetry in the space of bands is attributed to the difference in coupling constants V_1 and V_2. Assuming that only one of the b_i fields (with certain i) is condensed, we can simplify Eq. (15) to

$$-2iT\sum_n\frac{\Gamma_i(i\epsilon_n)}{i\epsilon_n-\epsilon_R+\mu+iN_a\varphi_i\Gamma_i(i\epsilon_n)}+\lambda=0. \tag{16}$$

The same result could be obtained as a result of the saddle-point equation $\delta F/\delta b_i(\tau)=0$, with the use of Eq. (6), assuming $b_i=\mathrm{const}$.

The constraint (5) follows from the analogous saddle-point approximation with respect to the λ field, $\delta F/\delta\lambda(\tau)=0$, which gives Eq. (5) in the form

$$2N_mT\sum_n\frac{1}{i\epsilon_n+\epsilon_R-\mu-iN_a\varphi_i\Gamma_i(i\epsilon_n)}+N_aN_m\varphi_i=1, \tag{17}$$

with the hole Green function of the localized state in the first term and $N_m=(2l+1)$ for the number of orbital states. The set of equations (16) and (17) determines φ_i and λ and, consequently, the impurity-level position and width in the mixed-valence state.

It should be noted that the renormalization of the free carrier Green function G_{ki} can be neglected, provided that we consider only one impurity. In the case of a finite impurity concentration, the correction is proportional to the impurity concentration, which we assume to be small.

As a next step, we calculate $\Gamma_i(z)$, which enters these equations. For complex frequencies z and for $\mu=0$, using Eqs. (9) and (13), we obtain

$$\Gamma_{1,2}(z)=i\int\frac{d^3k}{(2\pi)^3}w_0^2(k)V_{1,2}^2\frac{z\pm\Delta}{z^2-\Delta^2-v^2k^2}. \tag{18}$$

Let us denote $z=z_1+iz_2$ and take $w_0(k)=w_0=\text{const}$. After integrating along a contour in the upper half-plane of complex k, we have

$$\begin{aligned}\Gamma_{1,2}(z)=&\operatorname{sgn}(z_1z_2)\frac{w_0^2V_{1,2}^2}{4\pi v^3}(z_1\pm\Delta)^2\\&\times[(z_1^2-z_2^2-\Delta^2)^2+4z_1^2z_2^2]^{1/4}\\&\times\begin{cases}\sin\varphi, & z_1^2-z_2^2-\Delta^2<0,\\ \cos\varphi, & z_1^2-z_2^2-\Delta^2>0,\end{cases}\end{aligned} \tag{19}$$

where

$$\varphi=\frac{1}{2}\tan^{-1}\left|\frac{z_1z_2}{z_1^2-z_2^2-\Delta^2}\right|.$$

For $z_2\to0$ it simplifies to (here we restore the chemical potential μ)

$$\begin{aligned}\Gamma_{1,2}(z)=&\operatorname{sgn}[(z_1+\mu)z_2]\frac{w_0^2V_{1,2}^2}{4\pi v^3}(z_1+\mu\pm\Delta)\\&\times[(z_1+\mu)^2-\Delta^2]^{1/2},\quad |z_1+\mu|>\Delta,\end{aligned} \tag{20}$$

and $\Gamma_{1,2}(z)=0$, if $|z_1+\mu|<\Delta$.

The dependence of $\Gamma_{1,2}$ on energy is presented in Fig. 5 for the choice of parameters $V_1=1$, $V_2=0.2$, and $w_0=1.2\times10^{-11}\,\text{eV cm}^{3/2}$, at different values of the energy gap $\Delta=0.02$, 0.06, 0.10 eV. It clearly demonstrates the asymmetry in c and v bands, resulting in condensation of only the b_c field.

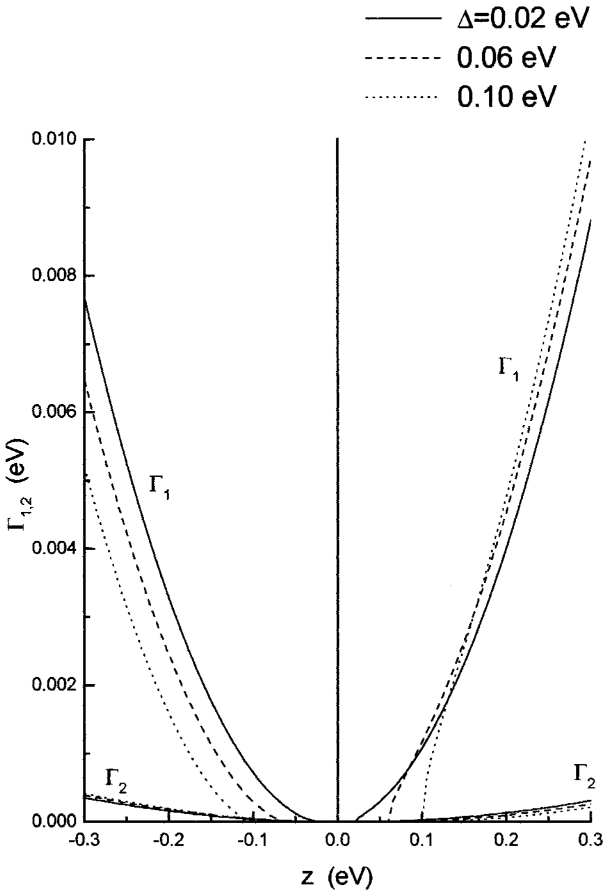

FIG. 5. Imaginary parts of the electron self-energy for the conduction (Γ_1) and valence (Γ_2) bands for different values of the energy gap.

IV. ENERGY OF THE IMPURITY LEVEL

The shift of the impurity energy level renormalized by hybridization is Re λ. We are going to find the singular part of energy shift that is strongly dependent on the electron spectrum of the host semiconductor. In order to do that, we need to solve Eqs. (16) and (17). A solution of Eq. (17) can be found easily for $T\to0$ [or, more exactly, for $T\ll N_a\varphi_i\Gamma(\epsilon_R-\mu)$]. The first term in Eq. (17) is the hole filling factor at the f center. At $T=0$ it can be written as

$$p_f=2N_m\int_{-\infty}^{0}\tilde{\rho}_f(E)dE, \tag{21}$$

where the spectral density is the imaginary part of the retarded Green function for holes, $\tilde{G}_f^R(E)$:

$$\tilde{\rho}_f(E)=-\frac{1}{\pi}\operatorname{Im}\tilde{G}_f^R(E). \tag{22}$$

We find

$$p_f=2N_m\begin{cases}\dfrac{1}{\pi}\tan^{-1}\left(\dfrac{N_a\varphi_i\Gamma_{i0}}{\mu-\epsilon_R}\right) & \text{for }\ \epsilon_R<\mu,\\[2ex] 1-\dfrac{1}{\pi}\tan^{-1}\left(\dfrac{N_a\varphi_i\Gamma_{i0}}{\epsilon_R-\mu}\right) & \text{for }\ \epsilon_R>\mu,\end{cases} \tag{23}$$

where we denoted $\Gamma_{i0}\equiv\Gamma_i(\epsilon_R-\mu)$.

The assumed constraint (5) and the single-loop approximation make our consideration valid for $N_m\gg1$ and $p_f\leqslant2$; so we get

$$p_f\simeq\frac{2N_aN_m\varphi_i\Gamma_{i0}}{\pi(\mu-\epsilon_R)}, \tag{24}$$

where we are restricted by the inequalities $N_a\varphi_i\Gamma_{i0}\ll\mu-\epsilon_R$ and $\mu>\epsilon_R$. In this region the renormalized level ϵ_R is always located below the Fermi energy, and its width $N_a\varphi_i\Gamma_{i0}$ is much smaller than the distance between this level and μ.

Using Eqs. (17) and (24), we get

$$N_aN_m\varphi_i\left(\frac{2\Gamma_{i0}}{\mu-\epsilon_R}+1\right)=1. \tag{25}$$

Thus, for $\Gamma_{i0}\ll\mu-\epsilon_R$ (no holes at the f center), we find

$$\varphi_i=1/(N_aN_m) \tag{26}$$

and, for $\mu-\epsilon_R\ll\Gamma_{i0}$ (the hole number is close to 1),

$$\varphi_i=\frac{1}{N_aN_m}\,\frac{\mu-\epsilon_R}{2\Gamma_{i0}}. \tag{27}$$

At finite temperatures, the modification of Eq. (21) is obvious:

$$p_f=2N_m\int f(E)\tilde{\rho}_f(E)dE, \tag{28}$$

where $f(E)=[\exp(E/T)+1]^{-1}$. For $N_a\varphi_i\Gamma_{i0}\ll T$, we find

$$p_f=2N_m[1-f(\epsilon_R-\mu)]. \tag{29}$$

This means that only the possibility of $(\mu-\epsilon_R)\gg T$ is allowed, since $N_m\gg 1$. It gives us

$$p_f=2N_m\exp\left(-\frac{\mu-\epsilon_R}{T}\right)$$

and

$$\varphi_i=\frac{1}{N_aN_m}\left[1-2N_m\exp\left(-\frac{\mu-\epsilon_R}{T}\right)\right]. \tag{30}$$

In a similar way we find the solution of Eq. (16). Writing it down in the form

$$\lambda=2iT\sum_n\Gamma_i(i\epsilon_n)G_f(i\epsilon_n),$$

using the spectral representation for G_f, and changing the summation over frequency to the contour integration Γ around the Im(z) axis in the complex z plane, we have

$$\lambda=-\frac{1}{\pi}\int_\Gamma dz\,f(z)\Gamma_i(z)\int_{-\infty}^{\infty}dE\,\frac{\rho_f(E)}{z-E}. \tag{31}$$

Using Eq. (18), we obtain

$$\lambda=-\frac{i}{\pi}\int_\Gamma dz\,f(z)\int_{-\infty}^{\infty}\frac{\rho_f(E)dE}{z-E}$$
$$\times\int\frac{d^3k}{(2\pi)^3}w_0^2V_{1,2}^2\frac{z+\mu\pm\Delta}{(z+\mu-E_k)(z+\mu+E_k)}. \tag{32}$$

In the integral over z, we can use the poles at $z=-\mu\pm E_k$, and in the integral over k, we transfer to the integration over E_k:

$$\frac{d^3k}{(2\pi)^3}\rightarrow\nu(E_k)dE_k,$$

with the density of states

$$\nu(E)=\frac{1}{2\pi^2v^3}E\sqrt{E^2-\Delta^2}.$$

Then we have

$$\lambda=-\frac{2}{\pi}\left(\int_{-\infty}^{-\Delta}+\int_{\Delta}^{\infty}\right)dE\,\frac{f(E-\mu)\Gamma_i(E-\mu)}{E-\epsilon_R+iN_a\varphi_i\Gamma_i(E-\mu)}, \tag{33}$$

where $\Gamma_i(E)$ is taken with $E\rightarrow E+i\delta$.

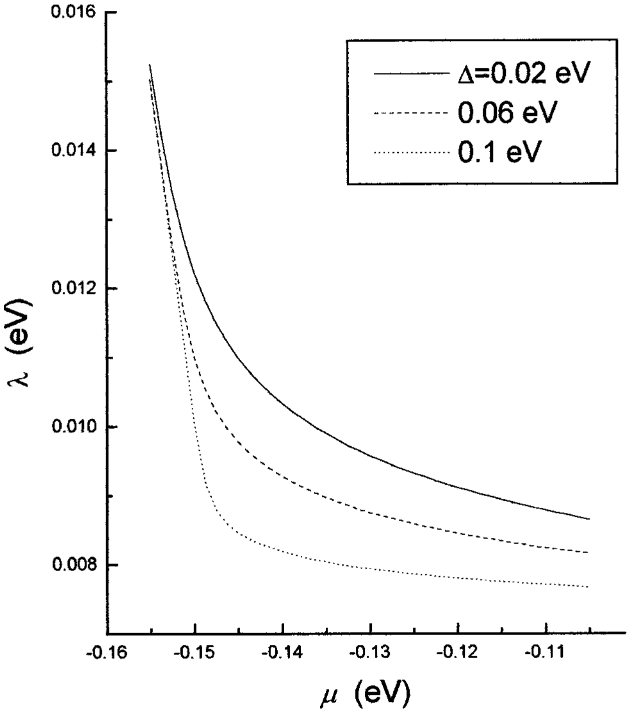

FIG. 6. Dependence of the impurity-level shift upon the chemical potential position for different values of the energy gap.

We assume that the chemical potential μ is located in the valence band, i.e., $\mu<-\Delta$ (and $T\ll\Delta$). Then Eq. (33) simplifies to

$$\lambda=-\frac{2}{\pi}\int_{-\Lambda}^{-\Delta}dE\,\frac{f(E-\mu)\Gamma_i(E-\mu)}{E-\epsilon_R+iN_a\varphi_i\Gamma_i(E-\mu)}, \tag{34}$$

where we have introduced a cutoff $\Lambda\simeq mv^2$; m stands for the contribution to the effective mass from remote bands.[13] It means that the energy Λ restricts the range of applicability of Dirac's model for the energy spectrum at large momenta.

At $T=0$ we obtain, from Eq. (34),

$$\lambda=-\frac{2}{\pi}\int_{-\Lambda}^{\mu}dE\,\frac{\Gamma_i(E-\mu)}{E-\epsilon_R+iN_a\varphi_i\Gamma_i(E-\mu)}. \tag{35}$$

This integral contains a regular part from $|\epsilon_R|<|E|<\Lambda$ and singular logarithmic contribution from the region near the Fermi energy, $\mu-\epsilon_R<|E|<|\epsilon_R|$. The result for singular part follows:

$$\lambda=\frac{2}{\pi}\Gamma_{i0}\ln\left(\frac{E_c}{\mu-\epsilon_R}\right), \tag{36}$$

where

$$E_c=|\epsilon_R|\exp\left(\frac{\Lambda^2}{|\epsilon_R\pm\Delta|\sqrt{\epsilon_R^2-\Delta^2}}\right).$$

This result is formally obtained for $T=0$. Since we consider the range $T\ll\mu-\epsilon_R$, the finite temperatures within this range do not change Eq. (36) as follows from calculations.

The results of numerical calculations of λ and φ_1 as functions of μ are shown in Figs. 6 and 7. Different energy gaps Δ in Figs. 6 and 7 may correspond to different compositions

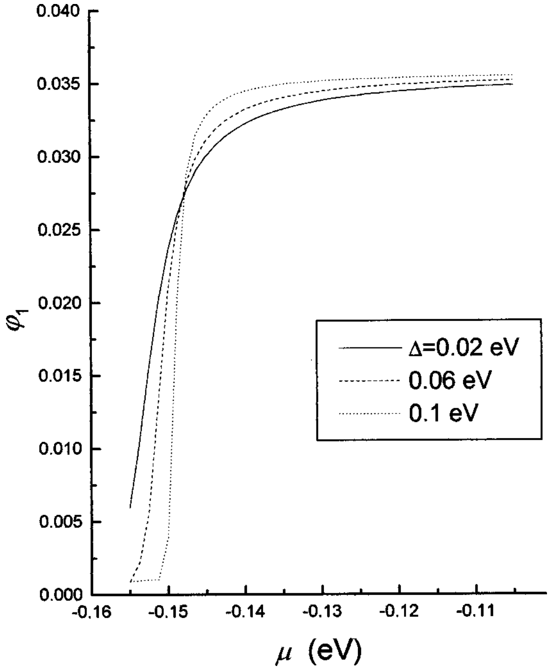

FIG. 7. Mean number of b bosons at the impurity level as a function of chemical potential position μ for different energy gaps.

in IV-VI ternary alloys. As follows from figures, the lower the gap is, the wider the region of μ is where intermediate valence takes place (valence changes since φ_1 changes from 0 to a maximum value). It is attributed to the indirect coupling of the impurity state with valence-band ones, via the intermediate conduction-band states. The impurity energy level follows μ when it moves inside the valence band (Fig. 6), and the width of the level depends strongly on μ in the mixed-valence region (Fig. 7). It is this many-particle level that is responsible for the properties of the rare-earth-doped narrow-gap semiconductor.

V. MAGNETIC SUSCEPTIBILITY

The magnetic moment of an impurity in magnetic field **H** oriented along the z axis can be calculated from

$$M_z = g^*\mu_B \int \rho(E)[f(E-\mu-g^*\mu_B H) - f(E-\mu+g^*\mu_B H)]dE, \tag{37}$$

where the effective g factor of our model g^* is determined by

$$g^{*2} = \mathrm{Sp}\sum_m (m^2+\sigma_z^2) = 2(2l+1)\left(\frac{l(l+1)}{3}+1\right) \tag{38}$$

and the impurity density of states

$$\rho_f(E) = \frac{1}{\pi}\frac{N_a\varphi_i\Gamma_{i0}}{(E-\epsilon_R)^2+(N_a\varphi_i\Gamma_{i0})^2}.$$

The static magnetic susceptibility, related to a single-impurity center (for many noninteracting centers, it should be multiplied by their number), is

$$\chi = \frac{\partial M_z}{\partial H} = -2g^{*2}\mu_B^2 \int \rho_f(E) f'(E-\mu)dE. \tag{39}$$

It gives, for $T \ll N_a\varphi_i\Gamma_{i0}$,

$$\chi = 2g^{*2}\mu_B^2\rho_f(\mu) \tag{40}$$

and, for $N_a\varphi_i\Gamma_{i0} \ll T$,

$$\chi = -2g^{*2}\mu_B^2\frac{\partial f(\epsilon_R-\mu)}{\partial\epsilon} = 2g^{*2}\mu_B^2\frac{1}{4T\cosh^2[(\epsilon_R-\mu)/2T]}. \tag{41}$$

If $\epsilon_R < \mu$ and $(\mu-\epsilon_R)/T \gg 1$, it simplifies to

$$\chi = \frac{2g^{*2}\mu_B^2}{T}\exp\left(-\frac{\mu-\epsilon_R}{T}\right). \tag{42}$$

Thus we find a different temperature behavior of the susceptibility for different temperature regions [Eqs. (40)–(42)].

VI. DISCUSSION

We have calculated the density of states of the many-particle resonance level ϵ_R near the Fermi energy, with a width $N_a\varphi_i\Gamma_{i0}$. The position of this level and its width depend on the chemical potential μ. The behavior of the resonance levels in IV-VI narrow-gap semiconductors differs in some aspects from that for simple metals with rare-earth impurities. First, the chemical potential in a semiconductor can be changed by doping with shallow impurities. No such effect is possible in metals. Second, the width of the resonance level is much less than the corresponding value in metals, due to the small density of states at the Fermi level for narrow-gap semiconductors. Actually, the width is not determined exactly by the electron density of states at the Fermi level (as it is in metals), but is described by Eq. (20), which is related to the more complicated energy band structure of IV-VI narrow-gap semiconductors.

We have restricted ourselves by considering only mean-field approximation theory. In our approach the fluctuations of b fields around the mean-field value is not so strongly suppressed, as for the large-spin theory. The formal reason for that is the absence of a large numerical factor in Eq. (14) for the polarization operator: the large number of valleys, N_a, only helps us to select the perturbation-theory diagrams containing the N_a factor. Thus the role of fluctuations remains a subject for further study.

ACKNOWLEDGMENTS

One of the authors (V.K.D.) is grateful to W. Dobrowolski and T. Story for useful discussions and to the Institute of Physics PAN for its hospitality. This work was supported in part by the Polish Commitee for Scientific Research, in particular under Grant No. 2 P03B 109 12.

[*] Present address: Electrical and Computer Engineering Department, Center of Quantum Devices, Northwestern University, Evanston, IL 60208.

[1] D. I. Khomskii, in *Quantum Theory of Solids*, edited by I. M. Lifshits (Mir, Moscow, 1982), pp. 70–129.

[2] T. V. Ramakrishnan, J. Magn. Magn. Mater. **63&64**, 529 (1987).

[3] D. T. Adroja and S. K. Malik, J. Magn. Magn. Mater. **100**, 126 (1991).

[4] P. Wachter, in *Handbook on the Physics and Chemistry of Rare Earths*, edited by K. A. Gschneider, Jr., L. Eyring, G. H. Lander, and G. R. Choppin (Elsevier, Amsterdam, 1994), Vol. 19, Chap. 132, pp. 177–382.

[5] D. K. Wohllenben, in *Valence Fluctuation in Solids*, edited by L. M. Falicov, W. Hanke, and M. B. Maple (North-Holland, Amsterdam, 1981), pp. 1–10.

[6] T. Story, M. Gorska, A. Lusakowski, M. Arciszewska, W. Dobrowolski, E. Grodnicka, Z. Golacki, and R. R. Galazka, Phys. Rev. Lett. **77**, 3447 (1996).

[7] E. Grodzicka, W. Dobrowolski, T. Story, E. I. Slynko, Yu. K. Vygranenko, M. M. H. Willekens, H. J. M. Swagten, and W. J. M. de Jonge, Acta Phys. Pol. A **90**, 801 (1996).

[8] I. Isber, C. Charar, F. Mahoukou, C. Fau, M. Averous, and Z. Glowacki, J. Cryst. Res. Technol. **31**, 701 (1996).

[9] N. Read and D. M. Newns, J. Phys. C **16**, 3273 (1983).

[10] D. M. Newns and N. Read, Adv. Phys. **36**, 799 (1987).

[11] P. Coleman, Phys. Rev. B **29**, 3035 (1984).

[12] P. Coleman, Phys. Rev. B **35**, 5072 (1987).

[13] G. Nimtz and B. Schlicht, in *Narrow-Gap Semiconductors* (Springer, Berlin, 1983), pp. 1–117.

[14] B. Ya. Moizhes and I. A. Drabkin, Fiz. Tverd. Tela (Leningrad) **25**, 1974 (1983) [Sov. Phys. Solid State **25**, 1139 (1983)].

[15] B. A. Volkov and O. M. Ruchaiskii, Pis'ma Zh. Eksp. Teor. Fiz **62**, 205 (1995) [JETP Lett. **62**, 217 (1995)].

[16] A. L. Shelankov, Solid State Commun. **62**, 327 (1987).

[17] A. A. Abrikosov, L. P. Gor'kov, and I. E. Dzyaloshinsky, *Quantum Field Theoretical Methods in Statistical Mechanics* (Dover, New York, 1975).